

# Hard turning of hot work steel AISI H11: Evaluation of cutting pressures, resulting force and temperature

**B. Fnides, M. A. Yallese, H. Aouici**

*Mechanics and Structures Laboratory (LMS), Department of Mechanical Engineering, May 08th 1945 University, Guelma 24000, Algeria, E-mail: fbrahim@yahoo.fr*

## Nomenclature

$a_p$  - depth of cut, mm;  $f$  - feed rate, mm;  $F$  - resulting cutting force, N;  $HRC$  - Rockwell hardness;  $K_a$  - axial cutting pressure, MPa;  $K_r$  - radial cutting pressure, MPa;  $K_v$  - tangential cutting pressure, MPa;  $R^2$  - coefficient of determination;  $VB$  - flank wear, mm;  $v_c$  - cutting speed, m/min;  $\alpha$  - relief angle, degree;  $\gamma$  - rake angle, degree;  $\lambda$  - inclination angle, degree;  $T$  - temperature, Celsius degree;  $\chi$  - major cutting edge angle, degree.

## 1. Introduction

Hard turning is a cutting process defined as turning materials with hardness higher than 45 HRC under appropriate cutting tools and high cutting speed. Machining of hard steel using advanced tool materials, such as mixed ceramic, has more advantages than grinding or polishing, such as short cycle time, process flexibility, compatible surface roughness, higher material removal rate and less environment problems without the use of cutting fluid. High-speed machining of dies and molds in their hardened state has become a normal practice in industry because it increased productivity and reduced energy consumption [1-3].

Cutting pressures and resulting force influence the deformation of the machined workpiece, its dimensional accuracy, the formation of chip and the tool nose.

In cutting process, the part, the cutting tool and the chip warm up, i.e. in cutting zone. The temperature increases, which is due to mechanical energy conversion into thermal energy because of elastic strain friction of the chip on rake and relief surfaces of the tool. The knowledge of the variation in temperature in the entire insert and particularly to the interface tool chip will allow a better adequacy between the cutting parameters, the characteristics of material to be machined like those of the tool [4-6].

## 2. Experimental procedure

The material used for the experiments is grade AISI H11 steel, hot work steel which is popularly used in hot form pressing. Its resistance to high temperature, its tenacity, its aptitude for polishing and its impact resistance thermal properties enable it to answer to the most severe requests in hot dieing and moulds under pressure [7, 8]. Its chemical composition is given in Table 1.

The workpiece is of 400 mm length and 75 mm in diameter. It is hardened to 50 HRC. Its hardness was measured by a digital durometer DM2D. The lathe used for machining operations is TOS TRENCIN; model SN40C, spindle power 6.6 kW. The cutting insert used is a mixed

ceramic (CC650 of chemical composition 70%Al<sub>2</sub>O<sub>3</sub>+30%TiC), removable, of square form having designation SNGN 120408 T01020.

Table 1

Chemical composition of grade AISI H11 steel

Composition	(wt. %)
C	0.35
Cr	5.26
Mo	1.19
V	0.5
Si	1.01
Mn	0.32
S	0.002
P	0.016
Other components	1.042
Fe	90.31

The toolholder adapted is of designation CSBNR2525M12 with geometry of the active part characterized by the following angles:  $\chi = 75^\circ$ ;  $\alpha = 6^\circ$ ;  $\gamma = -6^\circ$ ;  $\lambda = -6^\circ$  [9]. A pyrometer with infra-red models Raynger 3I was adapted to measure maximum temperatures in cutting zone.

## 3. Experimental results and discussion

### 3.1. Effect of feed rate on cutting pressures and on resulting force

Fig. 1 presents the evolution of cutting pressures according to the feed rate.

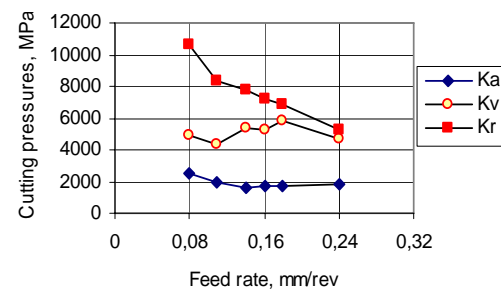


Fig. 1 Cutting pressures vs. feed rate at  $v_c = 125$  m/min;  $a_p = 0.15$  mm

It is noticed that with the increase in feed rate, the cutting pressures decrease. For weak feed rates, we record extremely high pressures. With the feed rate of 0.08 mm/rev, the cutting pressures  $K_a$ ,  $K_v$  and  $K_r$  are about

2521; 4870 and 10667 MPa. For the feed rate of 0.24 mm/rev, the pressures fall successively from 25.26; 3.78 and 50.49%. It is the radial cutting pressure which is the most affected.

Fig. 2 presents the evolution of resulting cutting force according to the feed rate. The effects on the practice plan are as follows: the increase in feed rate from 0.08 to 0.14 mm/rev increases the resulting cutting force from 38.92%. Increase in the feed rate from 0.08 to 0.24 mm/rev, leads to the rise in resulting cutting force from 82.78%.

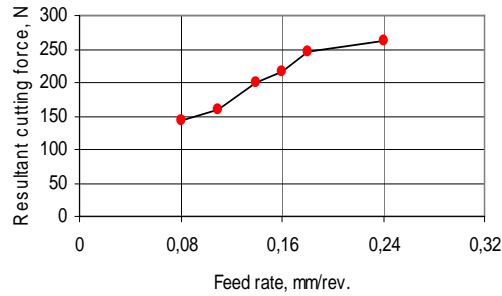


Fig. 2 Effect of feed rate on resulting cutting force at  $v_c = 125$  m/min;  $a_p = 0.15$  mm

### 3.2. Effect of cutting speed on cutting pressures and on resulting force

Fig. 3 shows the evolution of the cutting pressures according to the cutting speed. It arises that this evolution is carried out in three distinct zones.

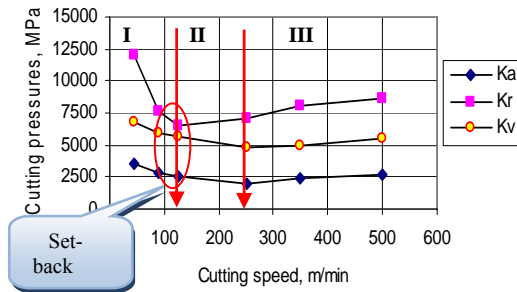


Fig. 3 Cutting pressures vs. cutting speed at  $a_p = 0.15$  mm;  $f = 0.08$  mm/rev

The first zone is decreasing. It extends the cutting speed from 45 to 125 m/min. the maximum values of the cutting pressures  $K_a$ ,  $K_t$  and  $K_r$  are about 3524; 6789 and 12044 MPa. These last are recorded at the cutting speed of 45 m/min. The end of this zone leads to the determination of the minimal speed of the field of application of the couple tool matter. The second is characterized by an interval where the cutting pressures are stabilized, unhooking is carried out starting from  $v_c = 125$  m/min. In practice, this zone constitutes the optimal range of use of the cutting edge. That causes to minimize the constraints which cause the requests and abrupt rupture of the cutting edge. The third zone starts when a speed  $v_c \geq 250$  m/min; curves of the cutting pressures take an ascending form because of the vibrations.

Fig. 4 illustrates the evolution of the resulting cutting force according to the cutting speed. By analyzing the shape of this curve, we note that the resulting force decreases until the speed of 125 m/min, beyond this limit, it

stabilizes oneself slightly. A rise in cutting speed from 45 to 125 m/min, leads to the reduction in resulting force from 36.70%. For the speed of 500 m/min, resulting force reaches only 74.44% of its maximum value.

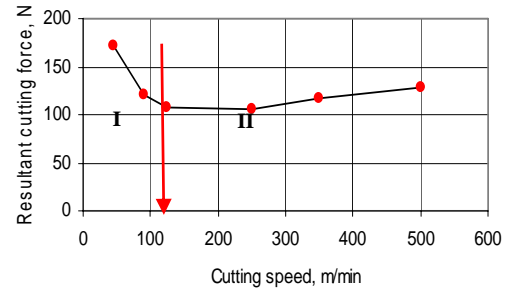


Fig. 4 Effect of cutting speed on resulting cutting force at  $f = 0.08$  mm/rev;  $a_p = 0.15$  mm

### 3.3. Effect of cutting depth on cutting pressures and on resulting force

Fig. 5 illustrates the evolution of the cutting pressures according to the depth of cut. It is noticed that the increase in cutting depth leads to a fall of the cutting pressures and that in two different periods of evolution. The first decreasing zone corresponds to an enormous loading of the cutting edge. The recorded pressures are very high in this zone, as an example, for a depth of 0.10 mm, we record pressures  $K_a$ ,  $K_v$  and  $K_r$  about 4504, 7725 and 21844 MPa. With the increase in cutting depth to 0.2 mm, the cutting pressures fall successively from 30; 21 and 41.5%. The second zone is characterized by the stability of axial and tangential cutting pressures. Radial cutting pressure continues its decrease until the depth of cut of 0.5 mm then it is stabilized. In short, it is misadvised working with low depths of cut because the cutting edge undergoes enormous pressures which cause and accelerate its damage.

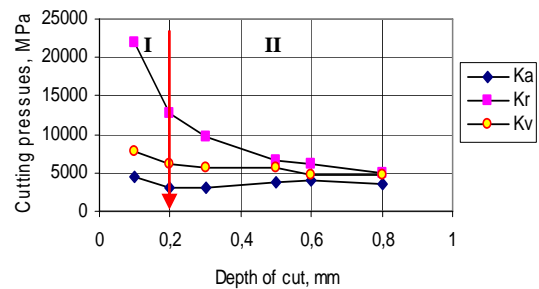


Fig. 5 Cutting pressures vs. depth of cut at  $v_c = 125$  m/min;  $f = 0.08$  mm/rev

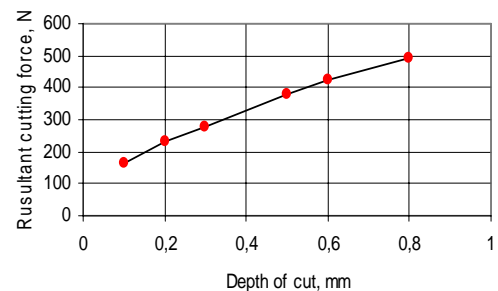


Fig. 6 Effect of cutting depth on resulting cutting force at  $v_c = 125$  m/min;  $f = 0.08$  mm/rev

The curve of Fig. 6 illustrates the evolution of the resulting cutting force according to the depth of cut. The variation depth of cut from 0.1 to 0.8 mm leads to the increase in resulting cutting force from 199.97%, this increase is almost linear. Depth of the cut seems to influence resulting cutting force more significantly than cutting speed and feed rate.

### 3.4. Effect of feed rate on cutting temperature

Fig. 7 shows the change of temperature in cutting zone according to the feed rate for the machining time of 20 seconds.

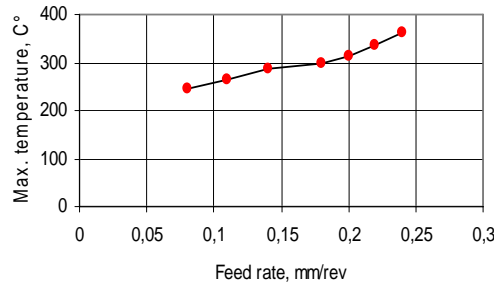


Fig. 7 Cutting temperature vs. feed rate at  $v_c = 125$  m/min;  $a_p = 0.15$  mm

With the increase in feed rate, section of the chip increases and consequently friction increases, this involves the increase in temperature. For a feed rate from 0.08 to 0.24 mm/rev, we record temperatures which vary from 246 to 363°C. It represents an increase of 48%.

### 3.5. Effect of cutting speed on cutting temperature

Fig. 8 highlights the effect of cutting speed on maximum temperature in the cutting zone for the machining time of 20 seconds. With the increase of the cutting speed, frictions increase, this induces an increase in temperature in the cutting zone. In this respect, the temperature measurement by infra-red pyrometer indicates that for a speed of 45 m/min, the maximum temperature is 182°C. For a cutting speed of 500 m/min, we record an increase in temperature in cutting zone of 182%.

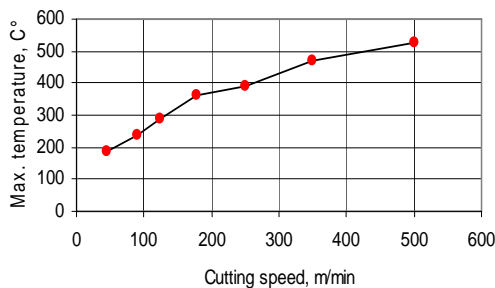


Fig. 8 Cutting temperature vs. cutting speed at  $a_p = 0.15$  mm;  $f = 0.08$  mm/rev

### 3.6. Effect of cutting depth on cutting temperature

Fig. 9 shows the change of the maximum temperature recorded in cutting zone as the function of cutting depth for the machining time of 20 seconds.

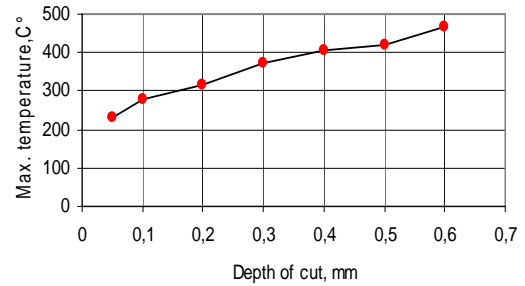


Fig. 9 Cutting temperature vs. depth of cut at  $v_c = 125$  m/min;  $f = 0.08$  mm/rev

For the cutting depth of 0.05 mm, the recorded temperature is 229°C. If the depth of cut increases to 0.4 mm (either 8 times), the value of temperature becomes 404°C, (or 1.76 times), which represents an increase in temperature of 76.41%. For the depth of cut of 0.6 mm, (either 12 times), the value of temperature reaches 467°C (or 2.04 times), we note an increase in temperature of 104%. If the depth of cut increases, the section of the chip increases and friction chip/tool increases what leads to an increase in temperature.

### 3.7. Effect of flank wear on cutting pressures

The curves (Fig. 10) present the evolution of cutting pressures according to flank wear ( $VB$ ). With the increase in flank wear, the forces of friction increase in their turn what generates additional pressures. The evolution of the cutting pressures according to flank wear is done in two stages. The first stage corresponds to a flank wear of 0.20 mm where the cutting pressures  $K_a$ ,  $K_v$  and  $K_r$  increase respectively 85; 36 and 184%. The second is characterized by a considerable increase in the radial pressure which has a harmful effect on the cutting edge. By comparing the values of components of the cutting pressure for a flank wear 0.105 with 0.44 mm, we note an increase in  $K_a$ ,  $K_v$  and  $K_r$  successively in 448; 107 and 621%. It is noticed that radial pressure is strongly affected by this phenomenon, followed by axial pressure, while the tangential pressure is less sensitive to this phenomenon.

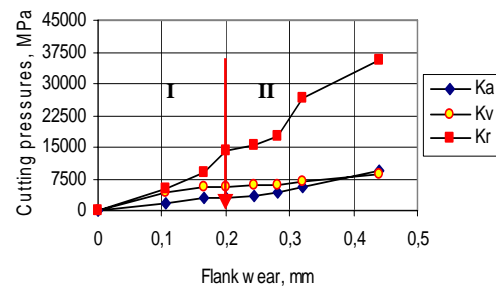


Fig. 10 Cutting pressures vs. flank wear at  $a_p = 0.15$  mm;  $v_c = 125$  m/min;  $f = 0.08$  mm/rev

## 4. Mathematical model of the influence of cutting regime on temperature

Table 2 presents the results of maximum temperature in cutting zone for various combinations of elements of cutting regime (feed rate, cutting speed and depth of cut) according to the multifactorial method.

Table 2 Acknowledgements

Temperature vs. various combinations of cutting regime elements

Tests N <sup>0</sup>	$f$ , mm/rev	$a_p$ , mm	$v_c$ , m/min	$T$ , C°
1	0.08	0.15	125	287
2	0.16	0.15	125	297
3	0.08	0.30	125	335
4	0.16	0.30	125	361
5	0.08	0.15	250	377
6	0.16	0.15	250	386
7	0.08	0.30	250	394
8	0.16	0.30	250	426

Treatment of these experimental results is defined by statistical mathematical model (Table 3).

To calculate the values of constants and the coefficient of determination  $R^2$  of this mathematical model, we used turbo Pascal program.

This model makes predictions to optimize the cutting process [10 - 13].

The detailed analysis of the found mathematical model (Table 3) confirms that the increased cutting speed leads to the increase in the temperature in cutting zone. The order of classification of the exponents of this determined model highlights the degree of influence of each factor of cutting regime on the maximum temperature. Indeed, cutting speed is the most influential factor.

Table 3  
Mathematical model of temperature vs. cutting regime

Mathematical model	Coef. of det.
$T = e^{4.702} f^{0.075} a_p^{0.177} v_c^{0.311}$	$R^2 = 0.948$

## 5. Conclusion

The tests of straight turning carried out on grade AISI H11 steel treated at 50 HRC, machined by a mixed ceramic tool (insert CC650) enabled us to study the influence of the following parameters: feed rate, cutting speed and depth of cut on cutting pressures, on resulting cutting force and on temperature in cutting zone. The impact of flank wear on cutting pressures is also studied.

It is to be noted that cutting pressures are very sensitive to the variation of cutting depth what affects especially the radial cutting pressure and the resulting force in a considerable way. It is also noted that cutting speed seems to influence temperature in cutting zone more significantly than the depth of cut and feed rate. Flank wear has a great impact on the evolution of cutting pressure components. Thus, the ranges of best cutting conditions adapted, were given.

Mathematical model deduced defined the degree of influence of each cutting regime element on the maximum temperature in cutting zone.

This study confirms that in dry hard turning of this steel and for all cutting conditions tested, the major pressure is the radial pressure.

The authors would like to thank Pr. Mohamed NEMAMCHA, President of the University of Guelma for his help and Mr. Mohamed AIB (Mamadou) for his participation in tests.

## References

1. **Chen, W.** Cutting forces and surface finish when machining medium hardness steel using CBN tools. -Int. J. of Machine Tools & Manufacture, 2000, 40, p.455-466.
2. **Qian, L., Robiul Hossan, M.** Effect on cutting force in turning hardened tool steels with cubic boron nitride inserts. -J. of Materials Processing Technology, 2007, 191, p.274-278.
3. **Fnides, B., Aouici, H., Yalles, M.A.** Cutting forces and surface roughness in hard turning of hot work steel X38CrMoV5-1 using mixed ceramic. -Mechanika. -Kaunas: Technologija, 2008, No.2(70), p.73-78.
4. **El-Wardany, T.I., Mohammed, E., Elbestawi, M.A.** Cutting temperature of ceramic tools in high speed machining of difficult-to-cut materials. -Int. J. Mach. Tools Manufact. 1996, v.36, No.5, p.611-634.
5. **Ay, H., Yang, W.J.** Heat transfer and life of metal cutting tools in turning. -Int. J. Heat transfer. 1998, v.41, No.3, p.613-623.
6. **Ren, X.J., Yang, Q.X., James, R.D., Wang, L.** Cutting temperatures in hard turning chromium hardfacings with PCBN tooling. -Journal of Materials Processing Technology, 2004, 147, p.38-44.
7. Site internet: <http://www.Buderus-steel.com>
8. Site internet: <http://www.premium-stahl.de/1.2343ESU>
9. SANDVIK Coromant, Catalogue Général : Tournage – Fraisage – Perçage – Alésage - Attachements, 2007.
10. **Ozel, T., Karpat, Y., Figueira, L., Paulo Davim, J.** Modelling of surface finish and tool flank wear in turning of AISI D2 steel with ceramic wiper inserts. - Journal of Materials Processing Technology, 2007, 189, p.192-198.
11. **Lima, J.G., Avila, R.F., Abrao, A.M., Faustino, M., Paulo Davim, J.** Hard turning: AISI 4340 high strength low alloy steel and AISI D2 cold work tool steel. -J. of Materials Processing Technology, 2005, 169, p.388-395.
12. **Oke, S.A., Oyedokun, O.I., Bamigbaiye, A.O.** Numerical analysis of temperature distribution of cold cylindrical metal subjected to machining. -Mechanika. -Kaunas: Technologija, 2006, No.1(57), p.48-54.
13. **Fnides, B., Aouici, H., Yalles, M.A.** Rugosité de surface et température en tournage dur de l'acier X38CrMoV5-1 usiné par une céramique mixte ( $Al_2O_3+TiC$ ). -2<sup>ème</sup> Congrès National de Mécanique, Constantine, 07-08 Avril 2008, F37.

B. Fnides, M.A. Yaltese, H. Aouici

PJOVIMO SLĖGIO, ATSTOJAMOSIOS JĖGOS IR  
TEMPERATŪROS NUSTATYMAS JĖGOS REŽIMU  
TEKINANT KAITRAI ATSPARŲ PLIENĄ AISI H11

Re z i u m ė

Darbo tikslas – nustatyti pjovimo slėgį, atstojamąją jėgą ir maksimalią temperatūrą jėgos režimu tekinant kaitrai atsparų plieną AISI H11. Šis 50 HRC kietumo nevolframinis Cr-Mo-V pagrindu sukurtas kaitrai ir dilimui atsparus plienas apdirbamas pjovimo įrankiu su kermetine plokšte CC650 (cheminė sudėtis 70% Al<sub>2</sub>O<sub>3</sub>+30% TiC). Jis naudojamas dideles apkrovas atlaikančių formų, liejamų slegiant, ilgaažių kietlydinio plokštelių, plastinių liejinių, veikiančių didelio slėgio, ir kaltų gamybai. Išilginio tekinimo bandymai buvo atlikti naudojant eksperimentų planavimo metodiką. Gauti rezultatai įgalino analizuoti pjovimo kintamųjų (pastūmos dydžio, pjovimo greičio ir gylio), veikiančių pjovimo zonoje, įtaką pjovimo slėgiui, atstojamajai jėgai ir temperatūrai. Taip pat nagrinėta įrankio antgalio nusidėvėjimo (*VB*) priklausomybė nuo pjovimo slėgio. Siekiant nustatyti kiekvieno pjovimo režimo elemento įtaką temperatūros maksimumui, buvo sudarytas matematinis modelis. Pagal jį parinktas geriausių pjovimo sąlygų diapazonas.

Šie tyrimai patvirtino, kad įvairiomis bandymo sąlygomis sausiai tekinant šį plieną didžiausias slėgis veikia radialine kryptimi.

B. Fnides, M.A. Yaltese, H. Aouici

HARD TURNING OF HOT WORK STEEL AISI H11:  
EVALUATION OF CUTTING PRESSURES,  
RESULTING FORCE AND TEMPERATURE

S u m m a r y

The aim of this work is to evaluate cutting pressures, resulting force and maximum temperature in hard turning of hot work steel AISI H11. This steel is hardened to 50 HRC, machined by a mixed ceramic tool (insert CC650 of chemical composition 70% Al<sub>2</sub>O<sub>3</sub>+30%TiC), free from tungsten on Cr-Mo-V basis, insensitive to temperature changes and having a high wear resistance. It is employed for the manufacture of highly stressed diecasting moulds and inserts with high tool life expectancy, plastic moulds subject to high stress and forging dies. The tests of straight turning were carried out according to the method of planning experiments. The results made it possible to

study the influence of cutting variables (feed rate, cutting speed and depth of cut) on cutting pressures, on resulting force and temperature in cutting zone. The effect of flank wear (*VB*) on cutting pressures is also studied. Mathematical model was deduced to express the influence degree of each cutting regime element on the maximum temperature. Thus, the ranges of best cutting conditions adapted, were given.

This study confirms that in dry hard turning of this steel and for all cutting conditions tested, the major pressure is the radial pressure.

Б. Фнидес, М.А. Яллесе, Г. Аоуици

ОПРЕДЕЛЕНИЕ СИЛЫ ДАВЛЕНИЯ,  
РАВНОДЕЙСТВУЮЩЕЙ СИЛЫ И ТЕМПЕРАТУРЫ  
ПРИ ТОЧЕНИИ ЖАРОСТОЙКОЙ СТАЛИ AISI H11

Р е з ю м е

Цель работы – установить силу давления, равнодействующую силу и максимальную температуру при силовом точении жаростойкой стали AISI H11. Эта 50 HRC твердости безвольфрамовая, жаре и износу стойкая сталь, созданная на основе Cr-Mo-V, обрабатывается резцом с керметовой пластинкой CC650 (ее химический состав 70% Al<sub>2</sub>O<sub>3</sub>+30% TiC). Эта сталь используется для изготовления литейных форм для литья под давлением, работающих под высокими нагрузками, износостойких твердотельных пластин, пластичных сплавов, воздействуемых высоким давлением, и наконечников долота. Эксперименты по точению проводились по методу планирования экспериментов. Полученные результаты позволили анализировать влияние переменных точения (величины подачи, скорости и глубины точения), действующих в зоне резания, на силу давления, равнодействующую силу и температуру в той же зоне. Также исследован износ наконечника инструмента (*VB*) в зависимости от силы давления. С целью установления влияния режимов резания на максимальную температуру разработана соответствующая математическая модель. С ее помощью подобран наилучший диапазон режимов резания.

Исследования подтвердили, что при разных условиях сухого точения стали, главная составляющая силы давления направлена в радиальном направлении.

Received March 03, 2008

DOI: 10.5755/j02.mech.15096